

1 Sediment dynamics across gravel-sand transitions: Implications
2 for river stability and floodplain recycling

3 Elizabeth H. Dingle^{1,2}, Hugh D. Sinclair², Jeremy G. Venditti^{1,3}, Mikael Attal², Tim C.
4 Kinnaird⁴, Maggie Creed², Laura Quick², Jeffrey A. Nittrouer⁵ and Dilip Gautam⁶

5 *¹Department of Geography, Simon Fraser University, Burnaby, BC, Canada*

6 *²School of GeoSciences, University of Edinburgh, Edinburgh, EH8 9XP, UK*

7 *³School of Environmental Science, Simon Fraser University, Burnaby, BC, Canada*

8 *⁴School of Earth and Environmental Sciences, University of St. Andrews, St. Andrews, KY16 9AL,*
9 *UK*

10 *⁵Department of Earth, Environment and Planetary Sciences, Rice University, Houston, TX, USA*

11 *⁶Practical Action Consulting, Kathmandu 15135, Nepal*

12 **ABSTRACT**

13 The gravel-sand transition (GST) is commonly observed along rivers. It is characterized by an
14 abrupt reduction in median grain size, from gravel- to sand-size sediment, and by a shift in sand
15 transport mode from wash load-dominated to suspended bed material load. We document changes
16 in channel stability, suspended sediment concentration, flux and grain size across the GST of the
17 Karnali River, Nepal. Upstream of the GST, gravel-bed channels are stable over hundred to
18 thousand-year timescales. Downstream, floodplain sediment is reworked by lateral bank erosion,
19 particularly during monsoon discharges. Suspended sediment concentration, grain size and flux
20 reveal counterintuitive increases downstream of the GST. The results demonstrate a dramatic

21 change in channel dynamics across the GST, from relatively fixed, steep gravel-bed rivers with
22 infrequent avulsion to lower gradient, relatively mobile sand-bed channels. The increase in
23 sediment concentration and near-bed suspended grain size may be caused by enhanced channel
24 mobility, which facilitates exchange between bed and bank material. These results bring new
25 constraints on channel stability at mountain fronts, and indicate that temporally and spatially
26 limited sediment flux measurements downstream of GSTs are more indicative of flow stage and
27 floodplain recycling than of continental-scale sediment flux and denudation rate estimates.

28 **INTRODUCTION**

29 Downstream of mountain ranges, river bed sediment fines as channels flow onto lower gradient
30 and laterally unconstrained landscapes (Sternberg, 1875). Sediment fining is a key component of
31 sediment transport that underpins the dynamic nature of rivers, and is central to fluvial
32 geomorphology and the depositional record it constructs. Downstream fining is attributed to size-
33 selective sediment sorting (e.g. Ashworth and Ferguson, 1989; Paola et al., 1992a; Ferguson et al.,
34 1996) and the mechanical breakdown (abrasion) of particles (e.g. Parker, 1991; Attal and Lavé,
35 2006; Dingle et al., 2017). Rivers commonly exhibit an abrupt transition in bed grain size, from
36 gravel to sand, over a short downstream distance (e.g. Shaw and Kellerhals, 1982; Ferguson et al.,
37 1996), termed the gravel-sand transition (GST). The development of GSTs has been attributed to
38 a combination of size-selective sorting (e.g. Paola et al., 1992b; Wathen et al., 1995; Ferguson et
39 al., 1996; Seal et al., 1997; Parker and Cui, 1998), abrasion of particles (e.g. Jerolmack and
40 Brzinski, 2010) and abrupt changes in Reynolds number dependent sediment suspension
41 thresholds (e.g. Venditti and Church, 2014; Lamb and Venditti, 2016). There is no generally
42 accepted or universal theory for why GSTs develop.

43 Across GSTs, observed changes in channel morphology may help elucidate sediment
44 transport adjustments and hint at possible causal mechanisms. Upstream of the GST, channels are
45 typically mobile only at high flows (Dong et al., 2019). Downstream, channels are lower gradient
46 and generally lower energy environments, but can be highly mobile when transporting large
47 sediment loads (Montgomery et al., 1999). A reduction in channel gradient is also commonly
48 observed at the GST (Sambrook-Smith and Ferguson, 1995; Ferguson, 2003) which, for stable
49 channel conditions, should reduce sediment transport capacity. Progress in understanding how
50 sediment transport adjusts across GSTs is limited by a paucity of direct observations.

51 In this paper we test for changes in sediment transport and channel mobility across a GST
52 in the Karnali River, Nepal. We document sediment and channel dynamics at a range of time
53 scales, including daily (suspended sediment samples), decadal (channel migration rates and
54 patterns from satellite imagery) and century to millennia scales (dating of paleochannels). We
55 complement these observations with calculations of sediment entrainment thresholds and
56 frequency of bed mobility based on hydrological records to constrain timescales of channel
57 mobility.

58 **The Karnali River**

59 The Karnali basin has a drainage area of 43,000 km² at the Himalayan mountain front. Its climate
60 is dominated by the Indian summer monsoon between May and September, when the majority of
61 annual water and sediment discharge occurs (Sinha and Friend, 1994). At the mountain front, near
62 the town of Chisapani, the river exits a confined bedrock gorge and flows onto the alluvial Ganga
63 Plain where it bifurcates into two branches (Fig. 1). At moderate flow in August 2017 (~4,500
64 m³/s), discharge was observed to split between the two branches equally. The GST is ~40 km
65 downstream of the mountain front, where there is a gradient break in the longitudinal river profile

66 (Fig. DR1). Over a distance of approximately 5 channel widths, the river bed composition changes
67 from 85% gravel to >95% sand. The gravel reach gradient (0.001-0.002 m/m) is twice the sand
68 reach gradient.

69 **METHODS**

70 Suspended sediment concentration and grain size data were collected at 5 sampling locations (Fig.
71 1) at 4 or 5 different depths, using a horizontal Van Dorn sampler deployed from an inflatable
72 cataraft in August 2017 (Data Repository; Fig. DR2.1-2.5). Instantaneous sediment flux was
73 calculated using two methods to evaluate uncertainty. We first calculated flux as the product of
74 depth-averaged concentration and Acoustic Doppler Current Profile discharge measurement. We
75 also calculated suspended sediment flux from the Rouse equation (see Data Repository). We
76 regard the Rouse profile method as most reasonable as it uses the concentration data to estimate a
77 profile that roughly fits the observations at lower depths, but does not incorporate the local and
78 temporal variability inherent with measurements.

79 Paleochannels were identified on the Karnali fan (Fig. 1) and dated using optically
80 stimulated luminescence (OSL) to determine when the channel was last active within the main
81 channel network (see Data Repository). To constrain shorter-term rates of channel mobility,
82 satellite imagery was analyzed for a 10 and 16 km reach upstream and downstream of the GST,
83 respectively. Channel positions were mapped from images between 1984 and 2016 for the gravel-
84 bed reach, and between 1975 and 2016 for the sand-bed reach.

85 The discharges required to move sediment in the gravel and sand reaches were calculated
86 using a model based on the modified Chezy equation (Parker, 2004) and the Shields number (see
87 Data Repository). For gravel reaches, we use a slope-dependent critical Shield's number (Lamb et

88 al., 2008) and a value of 0.03 for sand reaches. Flood event return periods were calculated using
89 gauged flow data fitted to Gumbel and Log Pearson Type III distributions. This assumes a stable
90 climate over the time-intervals considered here (10^4 years) such that the magnitude of a given
91 return-interval discharge is approximately constant. Holocene climate records suggest that the
92 intensity of the Indian summer monsoon has gradually weakened over the past ~8 kyr, but has
93 been relatively stable since ~5 kyr (Gupta et al., 2005; Dixit et al., 2014). The return period of our
94 projected discharges may be under-estimated at $>10^3$ yr timescales.

95 Grain size measurements were taken from two gravel surfaces (Fig. DR4; ‘gravel bar’ and
96 ‘gravel bed’) near the bifurcation using photo counting (Attal and Lavé, 2006; Whittaker et al.
97 2011; see Data Repository). Measurements were made of sand samples below the GST from
98 material collected from the channel bed (T5) and an adjacent bank (Table DR3).

99 **RESULTS**

100 OSL dating of paleochannels on the gravel fan suggests that these reaches change location through
101 avulsion on timescales of 10^3 - 10^4 years (Fig. 1). This is consistent with satellite imagery showing
102 that the gravel channel belt position was stable between 1984 and 2016 (Fig. DR5.1). In contrast,
103 meander migration rates immediately downstream of the GST are up to ~450 m per year (Fig.
104 DR5.2).

105 Sand is transported throughout the year (Fig. 2A). Gravel that makes up the bar surfaces in
106 the gravel reach ($D_{50} = 65$ mm) is moved when discharge exceeds $\sim 5,100$ m³/s. This threshold is
107 exceeded annually based on discharge records. Coarser gravel ($D_{50} = 231$ mm) on the bed of the
108 dry bifurcation point requires a discharge of $\sim 31,500$ m³/s if the form drag correction (β) is 0.5,
109 which corresponds to a 1-in-7,000 year discharge (Fig. 2B). Increasing β to 0.6 reduces the

110 threshold to $\sim 23,500 \text{ m}^3/\text{s}$, which corresponds to a 1-in-500 year discharge. Values of β reported
111 for gravel-bed channels typically vary between 0.5 and 0.6 (Venditti and Church, 2014).

112 Suspended sediment samples were collected during a moderate monsoon flow ($4,500 \text{ m}^3/\text{s}$,
113 return interval ~ 1 year; Fig. 2b). In the gravel reach (T1 to T4), suspended sediment grain size
114 (Fig. 3A) shows a slight overall downstream decrease, and a less prominent reduction in
115 concentration (Fig. 3B). Both show minor variations with flow depth. In the sand reach (T5),
116 concentration and D_{50} are higher in the lower 20% of the water column compared to the gravel
117 reach and the vertical gradients are steeper (Fig. 3A & B). Suspended sand flux remains
118 comparable between the bifurcation and upstream of the GST at $\sim 0.3\text{-}0.4 \text{ Mt/d}$ (T2-4; Fig. 3C). In
119 the sand reach, the instantaneous sediment flux is an order of magnitude higher at $\sim 3.7\text{-}4.5 \text{ Mt/d}$.

120 **DISCUSSION**

121 **Changes in Channel Mobility**

122 Upstream of the GST there is minimal lateral migration of the channel belt across the floodplain.
123 Major changes in channel configuration in the gravel-bed portion of the river appear to be driven
124 by apex-avulsion (Leddy et al., 1993), where channel thalweg sinuosity drives inner-bend lateral
125 accretion and outer-bend erosion resulting in cycles of channel plugging and abandoned channel
126 re-occupation. OSL dating and calculations of threshold for gravel bed entrainment at the
127 bifurcation suggest timescales associated with channel avulsion are ~ 400 to 7,000 years. In
128 contrast, downstream of the GST, high rates of channel migration driven by lateral meander
129 migration are enhanced by the presence of a poorly consolidated, low clay-content floodplain
130 material that is devoid of deep-rooted vegetation. Even under low flow conditions, both bed and
131 bank material are mobilized, enhancing sand delivery to the bed and lower portion of the water

132 column. Anecdotally, during our 3-hour survey of site T5, we observed the adjacent sand bank
133 retreat by ~ 3 meters. The increase in D_{50} in the near bed sample at T5 may reflect the fact that
134 material eroded from the bank is coarser than the material carried in suspension through the gravel
135 reach at that time. These coarser sediments may have been transported and deposited under larger
136 flood discharges, in contrast to the conditions under which the channel was sampled. The coarser
137 grain sizes at T5 were absent from samples in T1-T4, suggesting this observation was unlikely a
138 simple function of grain size sorting associated with the development of a Rouse-like suspended
139 bed material profile. These combined results suggest that the location of the GST controls channel
140 migration of alluvial rivers downstream of the Himalayan and possibly other mountain fronts.

141 **Temporal Changes in Sediment Transport**

142 The absence of grain size or concentration gradients for profiles collected in the gravel reach
143 suggests that sand is transported here as wash load. The steep concentration and grain size
144 gradients at T5 are consistent with theoretical models indicating this material is sourced from the
145 bed (Rouse, 1936). The significant increase in sediment flux and grain size across the GST (T4 to
146 T5) coincides with observed changes in channel mobility. It is suggested that the augmented
147 sediment flux in the sand reach is sourced from the banks. The interpretation that sand is no longer
148 transported as wash load at T5, is consistent with wash load deposition patterns modelled by Lamb
149 and Venditti (2016), and direct observations from the Fraser River (Venditti and Church, 2014;
150 Venditti et al., 2019).

151 Mass continuity dictates that the increase in sediment concentration across the GST cannot
152 be a persistent feature, given the aggrading nature of the Ganga Plain (e.g. Dingle et al., 2016).
153 Our flux estimates are from moderate monsoonal flow conditions. During peak seasonal flow
154 conditions, shorter lived and more intense floods occur, during which pulses of sand would be

155 delivered out of the mountains and into the gravel reach. A further increase in suspended sand load
156 within the gravel reach is also expected due to the breakdown of the bed surface armor layer and
157 associated release of finer matrix material. As flow recedes, the gravel bed and banks are no longer
158 mobile and sand transport is reduced through the gravel-bed reach (Fig. 4). Downstream, the sand
159 channel is still capable of reworking flood flow deposits (even under lower flows) via lateral
160 channel migration. The increase in sediment grain size, concentration and instantaneous flux below
161 the GST likely reflects continuous reworking and intermittent cannibalization of bank material
162 deposited by past floods. This sediment is likely only translated a short distance before being
163 deposited on downstream point bars and integrated back into the bank as the channel migrates
164 laterally and the bank accretes vertically.

165 **Implications on Sediment Flux Estimates**

166 In many systems, cohesive bank material and root networks limit lateral migration but sediment
167 storage and recycling is observed (e.g. Venditti et al., 2015), suggesting that our observations are
168 not unique to the Karnali River. An increase in suspended sediment concentration has been
169 observed across the GST in the Fraser River, British Columbia (Venditti et al., 2015). Following
170 a peak spring freshet flow in June 2007, observations of suspended sediment across the Fraser
171 GST revealed that the total flux of sand (bed load and suspended load) increased downstream from
172 0.044 Mt/d to 0.127 Mt/d (Data Repository; Table DR4). However, unlike the Karnali, the Fraser
173 River is laterally constrained; the increase in sediment flux occurs because of changes in sand
174 storage across the GST under different flow stages. During high flows a thick deposit of sand, up
175 to 10 m thick, is mobilized at the upstream limit of the GST and diffused downstream. The storage
176 at the upstream limit has been observed to fill again as flow wanes (Venditti et al., 2015).

177 Both lateral channel migration and vertical filling and depletion of sand across the Karnali
178 and Fraser River GSTs is reflected by a counter-intuitive downstream increase in sediment flux
179 under moderate and high flow conditions, respectively. This highlights potential limitations in the
180 use of temporally limited, local sediment sampling downstream of mountain ranges when
181 calculating continental-scale sediment fluxes and denudation rate estimates. Sediment flux
182 estimates using comparable methods by Lupker et al. (2011) on the Ganga River at Harding
183 Bridge, Bangladesh, were 7.51 Mt/d under peak flow conditions (44,800 m³/s). Our measurements
184 collected under moderate monsoonal flow conditions (~2,000 m³/s) are >50% of this value, despite
185 the Karnali basin making up <5% of the Ganga catchment area upstream of Harding Bridge. Our
186 results indicate that downstream increases in suspended sediment concentration and grain size
187 arise due to remobilization of bank material through lateral migration, suggesting that sediment
188 flux measurements in such settings are enhanced by this process. To confirm, long-term records
189 capturing sediment flux under a range of flow conditions are required.

190 **ACKNOWLEDGEMENTS**

191 Data collection was funded through a NERC GCRF Building Resilience grant (NE/P015905/1) to
192 H.D.S. and an EPSRC GCRF Institutional grant (EP/P510944/1) to M.A. Sampling equipment
193 was lent by Ed Tipper and Bob Hilton. The RTK-GPS was loaned from the NERC Geophysical
194 Equipment Facility. We thank Practical Action Consulting, B. Sitaula, R. Wagle and G. Thapaliya
195 for help in the field and the Nepalese DHM for the provision of discharge data. Data analysis and
196 manuscript development was supported by an NSERC Discovery Accelerator Grant to J.V. We
197 thank Peter Wilcock, Doug Jerolmack and an anonymous reviewer for comments that have focused
198 this manuscript.

199 **REFERENCES CITED**

200 Ashworth, P.J., and Ferguson, R.I., 1989, Size-selective entrainment of bed load in gravel bed
201 streams: *Water Resources Research*, v. 25, p. 627–634, doi:[10.1029/WR025i004p00627](https://doi.org/10.1029/WR025i004p00627).

202 Attal, M., and Lavé, J., 2006, Changes of bedload characteristics along the Marsyandi River
203 (central Nepal): Implications for understanding hillslope sediment supply, sediment load
204 evolution along fluvial networks, and denudation in active orogenic belts, *in* Special Paper
205 398: Tectonics, Climate, and Landscape Evolution, Geological Society of America, v. 398,
206 p. 143–171, doi:[10.1130/2006.2398\(09\)](https://doi.org/10.1130/2006.2398(09)).

207 Dietrich, W.E., 1982, Settling velocity of natural particles: *Water Resources Research*, v. 18, p.
208 1615–1626, doi:[10.1029/WR018i006p01615](https://doi.org/10.1029/WR018i006p01615).

209 Dingle, E.H., Attal, M., and Sinclair, H.D., 2017, Abrasion-set limits on Himalayan gravel flux:
210 *Nature*, v. 544, p. 471–474, doi:[10.1038/nature22039](https://doi.org/10.1038/nature22039).

211 Dingle, E.H., Sinclair, H.D., Attal, M., Milodowski, D.T., and Singh, V., 2016, Subsidence control
212 on river morphology and grain size in the Ganga Plain: *American Journal of Science*, v. 316,
213 p. 778–812, doi:[10.2475/08.2016.03](https://doi.org/10.2475/08.2016.03).

214 Dixit, Y., Hodell, D.A., Sinha, R., and Petrie, C.A., 2014, Abrupt weakening of the Indian summer
215 monsoon at 8.2 kyr B.P.: *Earth and Planetary Science Letters*, v. 391, p. 16–23,
216 doi:[10.1016/j.epsl.2014.01.026](https://doi.org/10.1016/j.epsl.2014.01.026).

217 Dong, T. Y., Nittrouer, J. A., Il'icheva, E., Pavlov, M., McElroy, B., Czapiga, M., Ma, H., and G.
218 Parker, 2019, Roles of bank material in setting bankfull hydraulic geometry as informed by
219 the Selenga River delta, Russia: *Water Resources Research*, doi: [10.1029/2017WR021985](https://doi.org/10.1029/2017WR021985)

220 Ferguson, R., Hoey, T., Wathen, S., and Werritty, A., 1996, Field evidence for rapid downstream
221 fining of river gravels through selective transport: *Geology*, v. 24, p. 179–182,
222 doi:[10.1130/0091-7613\(1996\)024<0179:FEFRDF>2.3.CO;2](https://doi.org/10.1130/0091-7613(1996)024<0179:FEFRDF>2.3.CO;2).

223 Ferguson, R.I., 2003, Emergence of abrupt gravel to sand transitions along rivers through sorting
224 processes: *Geology*, v. 31, p. 159–162, doi:[10.1130/0091-
225 7613\(2003\)031<0159:EOAGTS>2.0.CO;2](https://doi.org/10.1130/0091-7613(2003)031<0159:EOAGTS>2.0.CO;2).

226 Gupta, A.K., Das, M., and Anderson, D.M., 2005, Solar influence on the Indian summer monsoon
227 during the Holocene: *Geophysical Research Letters*, v. 32, doi:[10.1029/2005GL022685](https://doi.org/10.1029/2005GL022685).

228 Jerolmack, D.J., and Brzinski, T.A., 2010, Equivalence of abrupt grain-size transitions in alluvial
229 rivers and eolian sand seas: A hypothesis: *Geology*, v. 38, p. 719–722, doi:10.1130/G30922.1.

230 Lamb, M.P., and Venditti, J.G., 2016, The grain size gap and abrupt gravel-sand transitions in
231 rivers due to suspension fallout: *Geophysical Research Letters*, v. 43, p. 2016GL068713,
232 doi:[10.1002/2016GL068713](https://doi.org/10.1002/2016GL068713).

233 Leddy, J.O., Ashworth, P.J., and Best, J.L., 1993, Mechanisms of anabranch avulsion within
234 gravel-bed braided rivers: observations from a scaled physical model: Geological Society,
235 London, Special Publications, v. 75, p. 119–127, doi:10.1144/GSL.SP.1993.075.01.07.

236 Lupker, M., France-Lanord, C., Lavé, J., Bouchez, J., Galy, V., Métivier, F., Gaillardet, J.,
237 Lartiges, B., and Mugnier, J.-L., 2011, A Rouse-based method to integrate the chemical
238 composition of river sediments: Application to the Ganga basin: *Journal of Geophysical
239 Research: Earth Surface*, v. 116, p. F04012, doi:10.1029/2010JF001947.

240 Montgomery, D.R., Panfil, M.S. and Hayes, S.K., 1999. Channel-bed mobility response to extreme
241 sediment loading at Mount Pinatubo. *Geology*, 27(3), pp.271-274.

242 Paola, C., Heller, P.L., and Angevine, C.L., 1992a, The large-scale dynamics of grain-size
243 variation in alluvial basins, 1: Theory: *Basin Research*, v. 4, p. 73–90, doi:[10.1111/j.1365-
244 2117.1992.tb00145.x](https://doi.org/10.1111/j.1365-2117.1992.tb00145.x).

245 Paola, C., Parker, G., Seal, R., Sinha, S.K., Southard, J.B., and Wilcock, P.R., 1992b, Downstream
246 Fining by Selective Deposition in a Laboratory Flume: *Science*, v. 258, p. 1757–1760,
247 doi:[10.1126/science.258.5089.1757](https://doi.org/10.1126/science.258.5089.1757).

248 Parker, G., and Cui, Y., 1998, The arrested gravel front: stable gravel-sand transitions in rivers
249 Part 1: Simplified analytical solution: *Journal of Hydraulic Research*, v. 36, p. 75–100,
250 doi:[10.1080/00221689809498379](https://doi.org/10.1080/00221689809498379).

251 Parker G., 1991, Selective Sorting and Abrasion of River Gravel. I: Theory: *Journal of Hydraulic
252 Engineering*, v. 117, p. 131–147, doi:[10.1061/\(ASCE\)0733-9429\(1991\)117:2\(131\)](https://doi.org/10.1061/(ASCE)0733-9429(1991)117:2(131)).

253 Parker G., 2004, 1D sediment transport morphodynamics with applications to rivers and turbidity
254 currents. E-book available from [http://vtchl. uiuc. edu/people/parkerg/morphodynamics_e-
255 book. htm](http://vtchl.uiuc.edu/people/parkerg/morphodynamics_e-book.htm).

256 Rouse H., 1936, Nomogram for the settling velocity of spheres: National Research Council
257 Committee on Sedimentation Publ. (1936), p. 57-64.

258 Sambrook Smith, G.H., and Ferguson, R.I., 1995, The Gravel-Sand Transition Along River
259 Channels: *Journal of Sedimentary Research*, v. 65(2), p.423-430.

260 Seal, R., Paola, C., Parker, G., Southard, J.B., and Wilcock, P.R., 1997, Experiments on
261 Downstream Fining of Gravel: I. Narrow-Channel Runs: *Journal of Hydraulic Engineering*,
262 v. 123, p. 874–884, doi:[10.1061/\(ASCE\)0733-9429\(1997\)123:10\(874\)](https://doi.org/10.1061/(ASCE)0733-9429(1997)123:10(874)).

263 Shaw, J., and Kellerhals, R., 1982, The composition of recent alluvial gravels in Alberta river
264 beds.: Alberta Research Council.

265 Sinha, R., and Friend, P.F., 1994, River systems and their sediment flux, Indo-Gangetic plains,
266 Northern Bihar, India: *Sedimentology*, v. 41, p. 825–845, doi:[10.1111/j.1365-
267 3091.1994.tb01426.x](https://doi.org/10.1111/j.1365-3091.1994.tb01426.x).

268 Sternberg, H., 1875, Untersuchungen aber Lungen-und Querprofil geschiefbefahrender Flasse:
269 *Zeitschrift far Bauwesen*, v. 25, p.483-506.

270 Venditti, J.G., and Church, M., 2014, Morphology and controls on the position of a gravel-sand
271 transition: Fraser River, British Columbia: *Journal of Geophysical Research: Earth Surface*,
272 v. 119, p. 2014JF003147, doi:[10.1002/2014JF003147](https://doi.org/10.1002/2014JF003147).

273 Venditti, J.G., Domarad, N., Church, M., and Rennie, C.D., 2015, The gravel-sand transition:
274 Sediment dynamics in a diffuse extension: *Journal of Geophysical Research: Earth Surface*,
275 v. 120, p. 2014JF003328, doi:[10.1002/2014JF003328](https://doi.org/10.1002/2014JF003328).

276 Venditti, J.G., Nittrouer, J.A., Allison, M.A., Humphries, R.P., and Church, M., 2019, Supply-
277 limited bedform patterns and scaling downstream of a gravel-sand transition: *Sedimentology*,
278 doi:[10.1111/sed.12604](https://doi.org/10.1111/sed.12604).

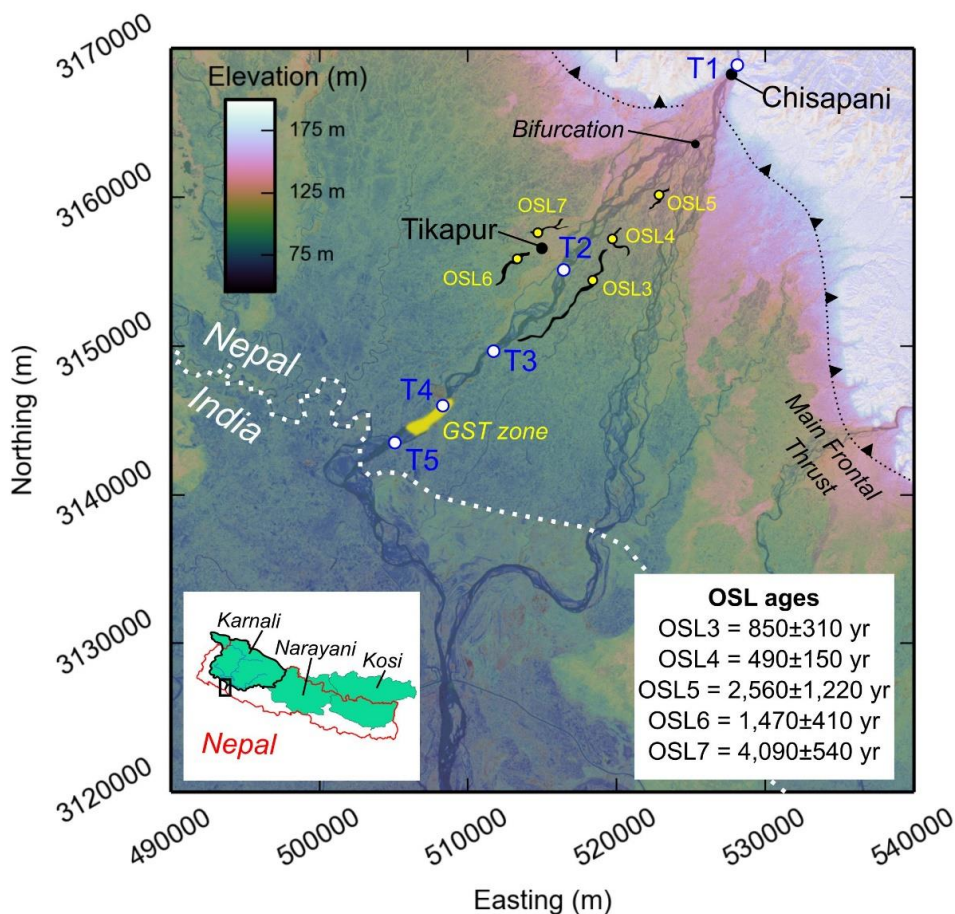
279 Wathen, S.J., Ferguson, R.I., Hoey, T.B., and Werritty, A., 1995, Unequal Mobility of Gravel and
280 Sand in Weakly Bimodal River Sediments: *Water Resources Research*, v. 31, p. 2087–2096,
281 doi:[10.1029/95WR01229](https://doi.org/10.1029/95WR01229).

282 Whittaker, A.C., Duller, R.A., Springett, J., Smithells, R.A., Whitchurch, A.L., and Allen, P.A.,
283 2011, Decoding downstream trends in stratigraphic grain size as a function of tectonic
284 subsidence and sediment supply: Geological Society of America Bulletin, v. 123, p. 1363–
285 1382, doi:[10.1130/B30351.1](https://doi.org/10.1130/B30351.1).

286 Yatsu, E., 1955, On the longitudinal profile of the graded river: Eos, Transactions American
287 Geophysical Union, v. 36, p. 655–663, doi:[10.1029/TR036i004p00655](https://doi.org/10.1029/TR036i004p00655).

288

289 **FIGURE CAPTIONS**



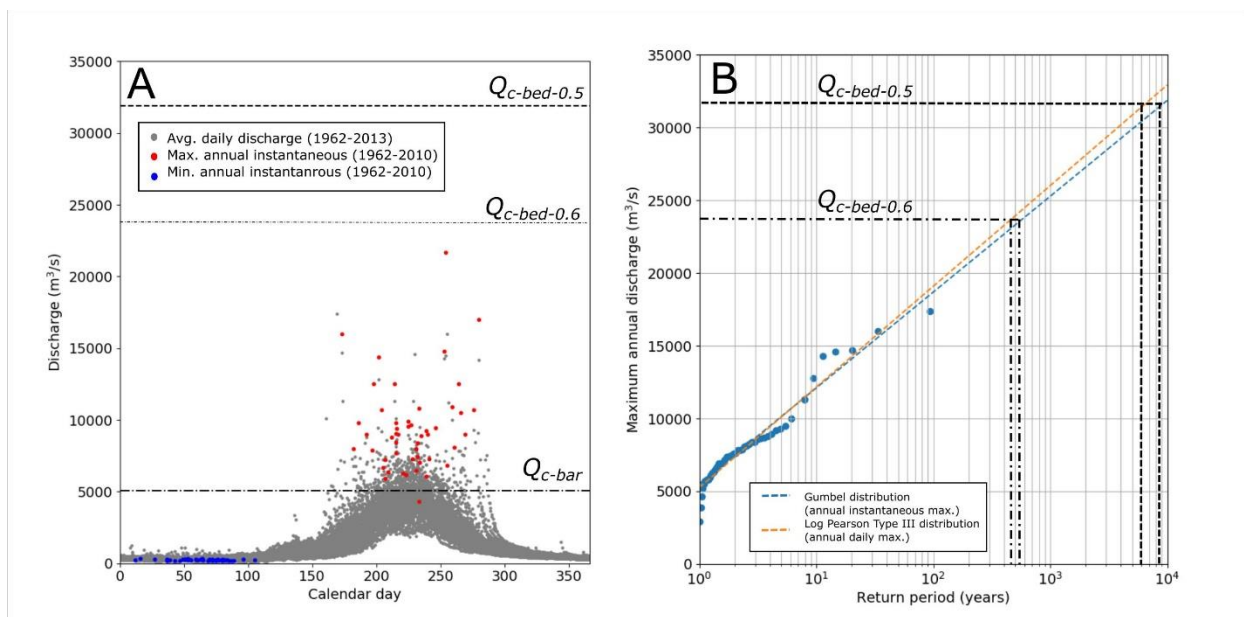
290

291 Figure 1. Study area showing suspended sediment sampling locations (T1-T5) and the gravel-sand
292 transition extension on the Karnali River. Paleochannels (black lines) on the fan and optically

293 stimulated luminescence dates are labelled (Data Repository for full methods). Data sources: 30
 294 m Shuttle Radar Topography Mission Digital Elevation Model (coordinates in UTM Zone 43N)
 295 and Sentinel-2 satellite imagery (October 26, 2016).

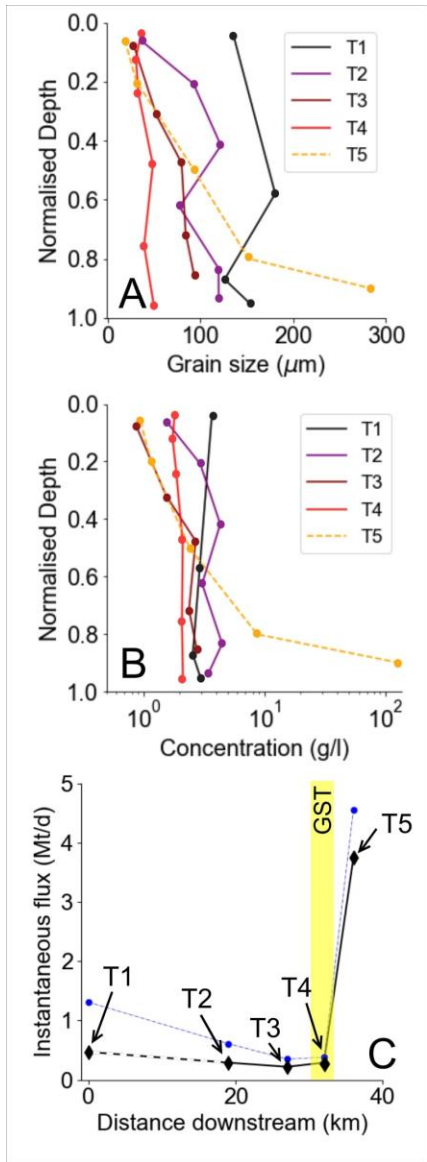
296

297



298

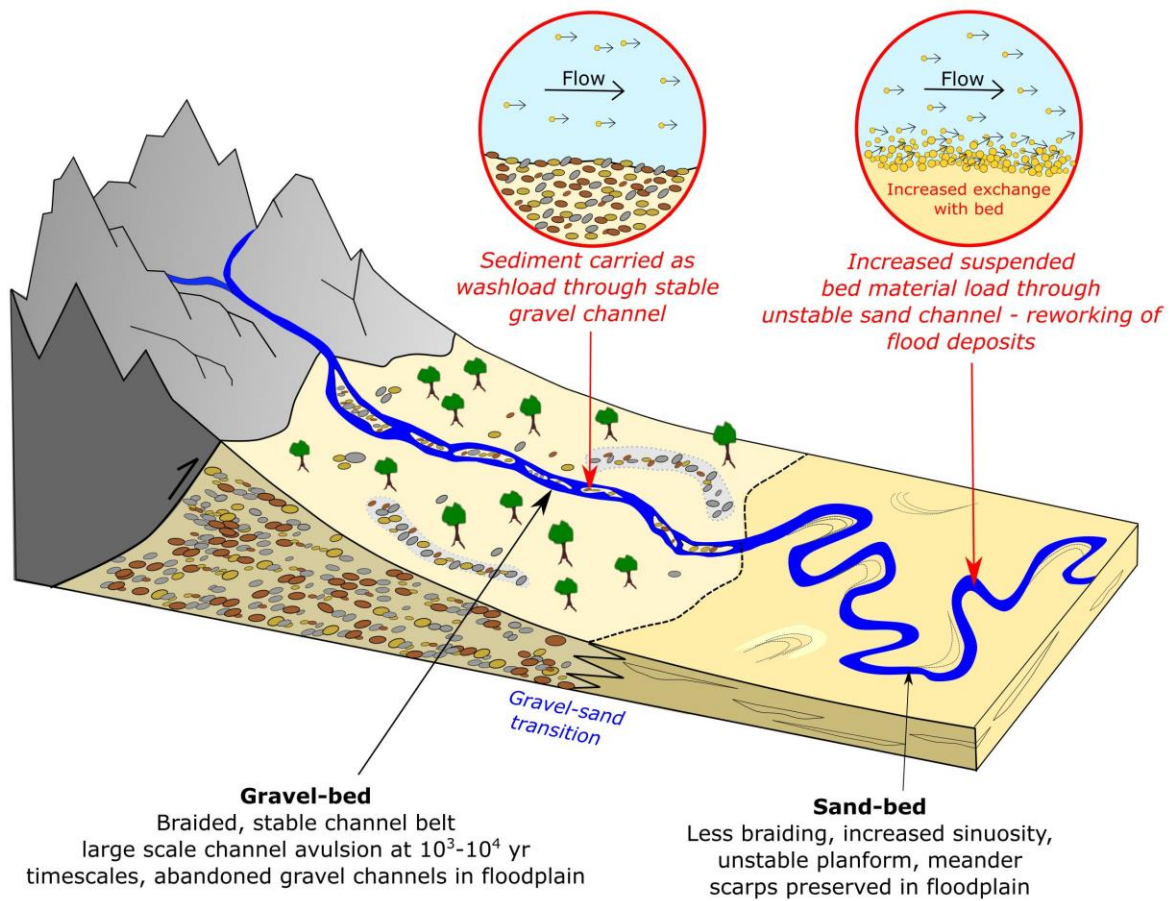
299 Figure 2. A) Discharge at Chisapani gauging station from 1962 to 2010. B) Projected return
 300 interval of discharges. Discharges required to mobilize the gravel-bar surface (Q_{c-bar}) and the
 301 median gravel-bed size at the bifurcation using $\beta=0.5$ ($Q_{c-bed-0.5}$) and $\beta=0.6$ ($Q_{c-bed-0.6}$), where β is
 302 the form drag correction used (see Data Repository), are shown. The discharge required to mobilize
 303 sand is 3-4 m³/s.



304

305 Figure 3. A) Median grain size at each vertical. B) Suspended sediment concentration at each
 306 vertical. C) Instantaneous sediment flux estimates. The black line and diamonds represent
 307 sediment fluxes calculated from depth-averaged Rouse profile concentrations, the blue circles and
 308 dashed lines represent fluxes calculated from depth-averaged measured concentrations. T1 is
 309 upstream of the bifurcation so some sediment is routed through the east branch before T2 (dashed
 310 line between T1 and T2). Channel depths are normalized: see Fig. DR2.1-2.5 for absolute depths.

311



312

313 Figure 4. Summary of changes in channel morphology, migration style (black text) and modes of

314 sediment transport (red text) across the Karnali gravel-sand transition under low to moderate flow

315 conditions.